PHYSICAL REVIEW B

CONDENSED MATTER

THIRD SERIES, VOLUME 51, NUMBER 10 1 MARCH 1995-II

Molecular-dynamics simulation of ferroelectric clusters

L. L. Boyer

Naval Research Laboratory, Complex Systems Theory Branch, Washington, D.C. 20375-5345

(Received 25 July 1994; revised manuscript received 4 November 1994)

Stoichiometric clusters with zero dipole moment are constructed from the perovskite structure by cleaving along the 8 ⟨111⟩ and 6 ⟨100⟩ planes positioned equal distances from an origin midway between the two cations. The procedure is used to form clusters of $NaCaF_3$, a hypothetical material which is predicted to be ferroelectric in the rigid-ion approximation. Results of molecular-dynamics calculations are reported for several clusters ranging in size from $N=35$ to 5900 ions. Calculations for the larger clusters were carried out on a massively parallel computer. A clear ferroelectric transition is observed for clusters with $N \gtrsim 800$.

I. INTRODUCTION

A ferroelectric crystal is, by definition, one that has a permanent polarization with two or more crystallographically equivalent orientations ($\mathbf{P}_i$) that can be switched from one to another by an electric field. At sufficiently high temperature ($T > T_c$) the polarization can fluctuate over all orientations. In other words, the crystal transforms to a high-temperature paraelectric phase with no permanent dipole moment, provided, of course, that T_c is less than the melting temperature. As the temperature is lowered through T_c, regions, or domains, corresponding to the various orientations ($\mathbf{P}_i$), form in the crystal. The formation of domains is partly entropy driven, but mainly the domains form to lower the electrostatic energy from what it would be in a single-domain crystal with no compensating surface charge. The amount of energy lowering can be as large as ~ 0.4 eV/atom for a ferroelectric like $BaTiO_3$ with a polarization of ~ 20 $\mu C/cm^2$. Producing a ferroelectric sample with predominantly one domain (poling) consists of supplying surface charge to produce an electric field that essentially cancels that due to the ferroelectric polarization.

The long-range nature of the forces involved in ferroelectric transitions and the large electrostatic energies driving domain formation suggest that surface effects are important in ceramic and/or film devices. One of the more interesting surface related effects in ferroelectrics is the depression of T_c with decreasing sample size for $BaTiO_3$ and $PbTiO_3$. The value of T_c for $BaTiO_3$ is lowered by ~ 100 K when the sample is ~ 0.15 μm, while a similar lowering of T_c for $PbTiO_3$ requires much smaller cluster sizes (~ 0.015 μm).[1] Why T_c should be so sensitive to cluster size, as in $BaTiO_3$, and why $PbTiO_3$ should be an order of magnitude less sensitive are not understood.

Several years ago Edwardson *et al.*[2] carried out molecular-dynamics (MD) calculations for a ferroelectric transition predicted in $NaCaF_3$. This included simulations for the bulk material, i.e., infinite crystals with periodic boundary conditions, and a cluster of $N=1080$ ions. Based on a comparison of thermal ellipsoids for interior atoms above and below the calculated bulk T_c, the cluster did appear to have a ferroelectric transition. This is somewhat surprising in view of the experimental results for $BaTiO_3$ and $PbTiO_3$. Thus, we decided to carry out a more comprehensive molecular-dynamics study of $NaCaF_3$ clusters to determine conclusively whether or not such small clusters can have ferroelectric transitions.

It would, of course, be most appropriate to carry out similar studies on $BaTiO_3$ for comparison. Unfortunately, this is not possible owing to the more complex electronic origin of ferroelectricity in these oxides. The ferroelectric instability in $BaTiO_3$ and similar compounds has been shown to derive from a rather complex electronic structure involving hybridized electrons with titanium d and oxygen p character.[3] Moreover, the instability is very sensitive to volume, so much so that the most accurate local-density-functional calculations can be substantially in error regarding the size of the instability at the predicted equilibrium volume.[4] On the other hand, structural instabilities in halide-based perovskites are easily described in terms of a rigid closed-shell electronic structure. Results obtained for halide-based systems, especially those for $NaCaF_3$, are interesting in their own right. While there are relatively few known ferroelectric halides, one ($BaMgF_4$) has been considered for thin-film applications.[5] The predictions for $NaCaF_3$ are considered reliable since similar calculations for existing related compounds, e.g., $KCaF_3$ (Ref. 2), $RbCaF_3$ (Ref. 6), and $CsCaF_3$ (Ref. 7) yield remarkably accurate structural predictions.

Calculations were carried out for several clusters with $N \leq 5900$. Parallel computation was used for the larger clusters and carried out on the CM-200 and CM-5 computers. In Sec. II we discuss the algorithm used for summing over pair interactions using a massively parallel computer. The potentials used to describe $NaCaF_3$ are described in Sec. III and a method for preparing stoichiometric clusters with no dipole moment in the paraelectric phase is described in Sec. IV. The results are reported and discussed in Sec. V and summarized in Sec. VI.

II. COMPUTATIONAL METHOD

Certain problems in molecular dynamics, e.g., the simulation of ionic clusters, require the sum over all pairs of atoms to determine forces with sufficient accuracy. A row-column difference method for summing over all pairs using a north-east-west-south (NEWS)-type configuration of processors was introduced by Boyer and Pawley.[8] In this method the position coordinates of two sets of atoms are spread across the rows and columns of two two-dimensional arrays (R and C). The difference between R and C is then the relative coordinates for all possible pairs between members of the two sets. Summing over all pairs of sets, with some minor alterations to avoid double counting and self-interactions, accounts for all pairs. Another approach discussed by Boyer and Pawley was the "ring" method, in which the position coordinates are placed in two singly dimensioned arrays. Repeated cyclic shifts of one array relative to the other then accounts for all pairs. The method employed here combines these two approaches by adding a third (vertical) dimension to the R and C arrays.

To illustrate this vertical-row-column difference algorithm, consider first a collection of 20 particles. The total number of distinct pairs, excluding self-interactions, is $20(20-1)/2=190$. Let us assume our R and C arrays are dimensioned $5\times4\times4$. Initially, the coordinates (x,y, or z) of particles 1–4 are spread across the top rows of R and the top columns of C, particles 5–8 across the second layer of R and C, . . . , and particles 17–20 across the bottom layers of R and C. Specifically, if we are dealing with the x components of the position vectors, then $R(l,i,j)=x_k$ where $k=4(l-1)+i$ and $C(l,i,j)=x_k$ where $k=4(l-1)+j$. The difference $D=R-C$ accounts for all relative x coordinates among particles 1–4 and themselves, among particles 5–8 and themselves, . . . , among particles 17–20 and themselves. At this point, of course, care must be taken to avoid double counting $[D(l,i,j)=-D(l,j,i)]$ and self-interaction $[D(l,i,i)=0]$. (See Ref. 3 for details.) With this consideration, six pairs are handled in each layer, for a total of 30. Next, the coordinates in either R or C, say C, are given a cyclic shift along the l index, so that $C(1,i,j)$ contains coordinates of particles 17–20, $C(2,i,j)$ contains coordinates of particles 1–4, . . . , $C(5,i,j)$ contains coordinates of particles 13–16. Now the difference D accounts for $5\times4\times4=80$ distinct pairs. A second cyclic shift and difference account for another 80 pairs. This includes all $30+80+80=190$ pairs. In general, the number of cyclic shifts required is $(L-1)/2$ if the number of layers (L) is odd, and $L/2$ if L is even. For L even, the bottom $L/2$ layers of the last cyclic shift account for the same pairs as the top $L/2$ layers, presenting another special case to consider in order to avoid double counting. If, for example, we had six layers (24 particles) the accounting of all $24(24-1)/2=276$ pairs would require four D matrices (three cyclic shifts) with 36, 96, 96, and 48 distinct pairs, respectively, for each D.

It is unlikely that the number of particles in any real cluster one wishes to consider will exactly fill the R and C arrays. However, this problem is easily handled by including enough dummy particles with coordinates that are "infinitely" far from the real cluster and from each other. Another consideration is the method for handling the various types of interactions that may be present. For example, the clusters of consideration in this paper ($NaCaF_3$) have six different types of interactions. This detail was handled by simply grouping the particles in a way such that each type of interaction was treated separately; that is, each D matrix pertained to only one type of interaction.

III. POTENTIALS

The pair potentials used for $NaCaF_3$ were derived following the method of Gordon and Kim:[9]

$$\varphi_{ij}(r)=\frac{Z_iZ_j}{r}+\sum_{k=1}^{4}\Phi_{ij}^{k}(r)\ ,$$

where Z_i are the ionic charges ($+1$, $+2$, and -1, respectively, for Na, Ca, and F), the index k refers to the type of short-range interaction (short-ranged electrostatic, kinetic, exchange, and correlation, respectively) and are derived from the charge density of free ions. It is convenient to determine parameters of analytic functions which give a reasonably good fit to numerical values for $\Phi_{ij}^{k}(r)$ at selected values of r, and then use the analytic form in the MD simulation. In our calculations a simple exponential form was used for each k,

$$\Phi_{ij}^{k}(r)=\alpha_{ij}^{k}\exp(-\beta_{ij}^{k}r)\ .$$

The total interactions for Na-Na, Na-Ca, and Ca-Ca pairs are sufficiently dominated by the ionic term, for ranges of r of interest in our calculation, that we exclude the short-range interactions for these pairs. The α and β parameters used for the Ca-F and F-F interactions are listed in Ref. 6 while the parameters for the Na-F interactions are listed in Ref. 10.

Bulk calculations, i.e., calculations for the infinite solid with periodic boundary conditions, using these potentials, give a ferroelectric ground state which is 0.13 eV/unit cell lower than the corresponding static structure constrained to that of the paraelectric phase. (In this case one unit cell is two formula units.) Molecular-dynamics calculations for the bulk crystal place the ferroelectric transition temperature at $\sim$500 K.[11] Previous calculations were performed using a more accurate parametrization of the Gordon-Kim-derived numerical potentials.[12] Those results found a ferroelectric ground state 0.15

TABLE I. Stoichiometric clusters $n(NaCaF_3)$ which result from cleaving the perovskite structure (lattice constant a) along 14 planes ($\langle 111 \rangle$ and $\langle 100 \rangle$) a distance d_c from an origin midway between the two cations. All such clusters are listed for $n \leq 44$ as well as those of larger clusters chosen for simulation. The shell identification number is used in the analysis and presentation of simulation results.

Sequence number	n	d_c/a	Shell ID
1	1	0.4331	
2	4	0.7501	
3	7	1.0104	1
4	10	1.2501	
5	17	1.2991	
6	23	1.5878	
7	32	1.7501	
8	44	1.8764	2
14	160	3.0311	3
19	350	3.8972	4
25	717	5.0519	5
30	1180	5.9179	6

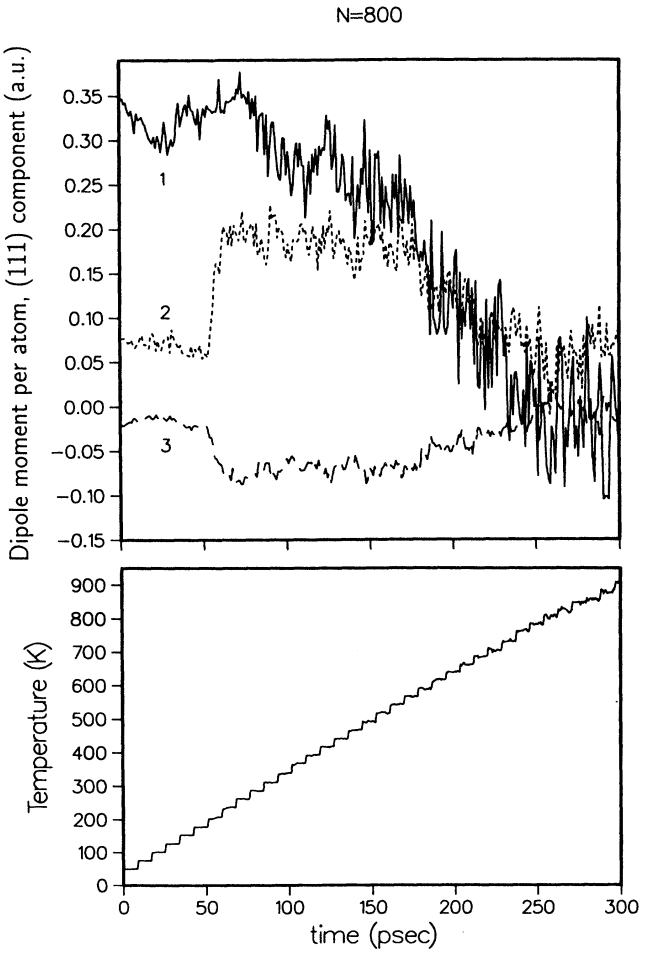

FIG. 1. The (111) component of the dipole moment per atom (atomic units) for each of the three shells (see Table I) of the 160 ($NaCaF_3$) cluster (upper panel) and the temperature (lower panel) as a function of simulation time.

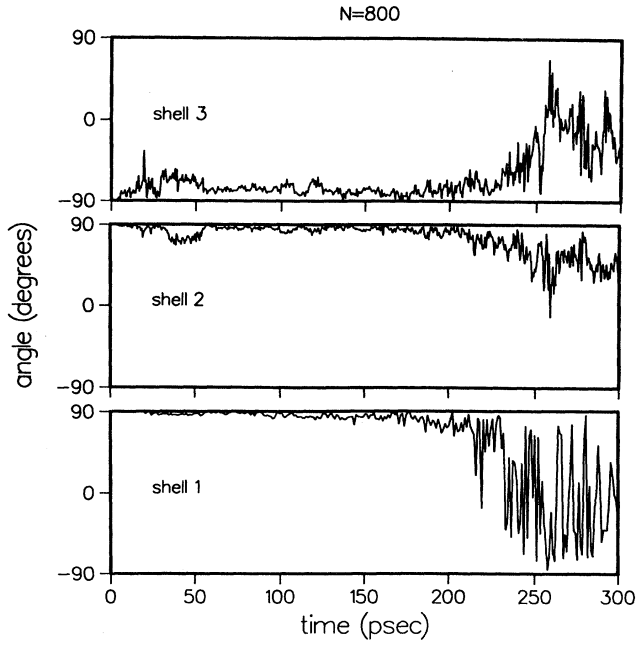

FIG. 2. Angle of the dipole moment of each shell of the 160 ($NaCaF_3$) cluster relative to the (111) axis as a function of simulation time [+90 corresponds to coincidence with the (111) direction].

eV/unit cell lower than the paraelectric phase[13] and a bulk ferroelectric transition temperature of ~ 550 K.[2]

IV. CLUSTER PREPARATION

Consider the ideal perovskite structure with a coordinate system whose origin is placed midway between the two cations, specifically at $(a/4, a/4, a/4)$ from either cation where a is the lattice constant. Now, if the crystal is cleaved on the 14 $\langle 111 \rangle$ and $\langle 100 \rangle$ planes equidistant (d_c) from the origin, then the clusters which result are stoichiometric, have C_{3v} symmetry, and no dipole moment. Some of the cluster sizes which result from this procedure are listed in Table I along with corresponding values of d_c.

This procedure for forming stoichiometric clusters with zero dipole moments from the ideal perovskite structure, clearly, can be applied to form clusters from a distorted perovskite structure, simply by cleaving the undistorted structure, and then, moving the atoms to their distorted positions.

The sequence of cluster sizes, $N = 35$, 220, 800, 1750, 3585, and 5900, determined from $d_c = 1.1a$, $2.1a$, $3.1a$, $4.1a$, $5.1a$, and $6.1a$, were selected for molecular-dynamics simulation. We denote the layer of atoms which is added to the $(i-1)$th cluster in this sequence, to form the ith cluster, the ith shell. For example, shell 3 corresponds to the 580 atoms which must be added to the $N = 220$ cluster to form the $N = 800$ cluster.

V. RESULTS

The *bulk* ferroelectric structure has an energy of 0.013 eV/atom *lower* than that of the paraelectric structure.

On the other hand, when a cluster is removed from the bulk, following the procedure given in Sec. IV, the ferroelectric structure has an ~ 0.36 eV/atom higher energy than the paraelectric structure, which is more than sufficient energy to melt the cluster. Thus, to avoid melting and/or major disruption of the prepared structure, the clusters first were rapidly quenched to remove the energy due to polarization. The structures obtained for the $N=35$ and 200 clusters were not immediately recognizable in terms of the bulk ferroelectric structure, and no further calculations were carried out on these smaller clusters. On the other hand, the interior of the larger clusters ($N \gtrsim 800$) evidently had a structure similar to that of the bulk ferroelectric, as indicated by the magnitude and direction of the dipole moment associated with the inner shells. The unrelaxed dipole moment is, in atomic units, 0.394 N.

The magnitude and direction of the dipole moment associated with the various shells of the clusters with $N=800$, 1750, 3585, and 5900 atoms are plotted in Figs. 1–8 with increasing simulation time. The temperature was increased in a stepwise fashion as indicated in the lower panels of Figs. 1, 3, 5, and 7. The magnitudes of the dipoles are shown in the upper panels of these figures while their directions, as indicated by the angles relative to the (111) axis, are plotted in Figs. 2, 4, 6, and 8.

There are some general features of the results shown in these figures that should be noted. (1) At low temperatures, the magnitude of the dipole moment per atom of the central region (interior shell or shells) is near that determined from a bulk calculation (0.394). (2) The total dipole moment of the cluster, which can be determined from the results in the figures by multiplying the magnitude per atom by the number of atoms and summing, is nearly zero for all times (temperatures). (3) As the time (temperature) increases the dipole moment of the central region decreases, until, at the transition its moment begins to fluctuate in sign along the (111) direction, averaging to zero as expected for a ferroelectric transition. These fluctuations can be seen in the plots of the (111) components of the dipole moment (e.g., upper panel of Fig. 7), but they are most evident in the plots of the dipole angle relative to the (111) axis (Figs. 2, 4, 6, and 8). (4) The transition temperatures are not very precisely determined from such simulations. However, the smaller clusters appear to have a transition temperature ~ 700 K, while that of the largest cluster is somewhat smaller

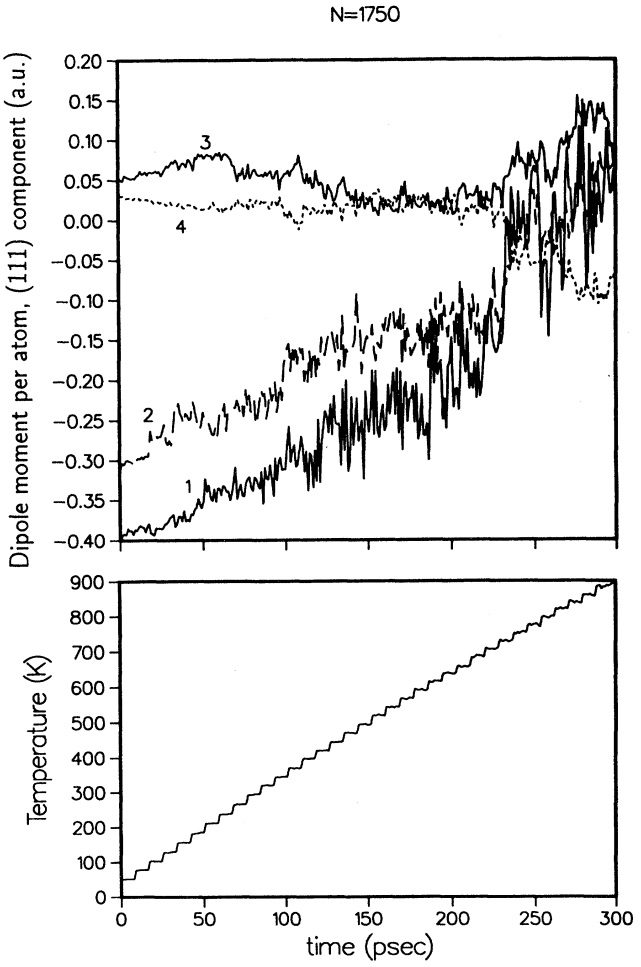

FIG. 3. The (111) component of the dipole moment per atom (atomic units) for each of the four shells (see Table I) of the 350 ($NaCaF_3$) cluster (upper panel) and the temperature (lower panel) as a function of simulation time.

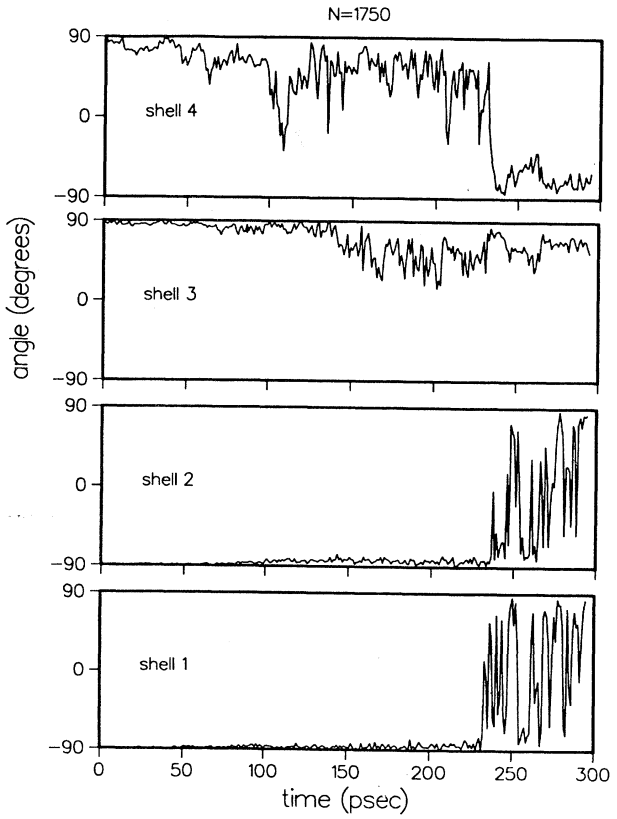

FIG. 4. Angle of the dipole moment of each shell of the 350 ($NaCaF_3$) cluster relative to the (111) axis as a function of simulation time [+90 corresponds to coincidence with the (111) direction].

(~630 K) and nearer to that obtained for a bulk calculation (~500 K). Now we consider the results of each cluster individually, pointing out unique features, such as domain patterns and wall motion, as well as some of the similarities already mentioned.

A. $N=800$

The quenched dipole moment per atom for shell 1 (~0.35) is near that of the bulk (0.394). The dipole moment of shell 2 is in the same direction as shell 1, while that of shell 3 is in the opposite direction. Thus, the cluster has an interior domain and a surface domain with opposite polarization. Notice that the total moment is nearly zero. After about 50 psec into the simulation an abrupt surface relaxation occurs which sharpens the transition between the two domains. At about 230 psec the temperature has been raised to ~700 K and the inner region clearly begins to fluctuate between the two polarization states, indicative of a ferroelectric transition.

B. $N=1750$

The results obtained for the 1750 atom cluster are similar to that of the 800 atom cluster. However, the quenched-in domain structure of the 1750 atom cluster proved to be more stable at low temperature. At least, no sudden rearrangement of surface atoms occurred below room temperature. Like the $N=800$ results, the magnitude of the interior dipole moment is close to that of the bulk, and once again, at about 700 K, the interior moments (shells 1 and 2), begin to fluctuate between the two states of polarization (+90 and −90 degrees in Fig. 4).

C. $N=3585$

The description for the 3585 atom cluster is very similar to that of the smaller clusters. In this case, however, the domain wall at low temperatures ($T<600$ K) moved nearer to the surface as time progressed, the wall started out between shell 3 and shell 4 (opposite dipole directions

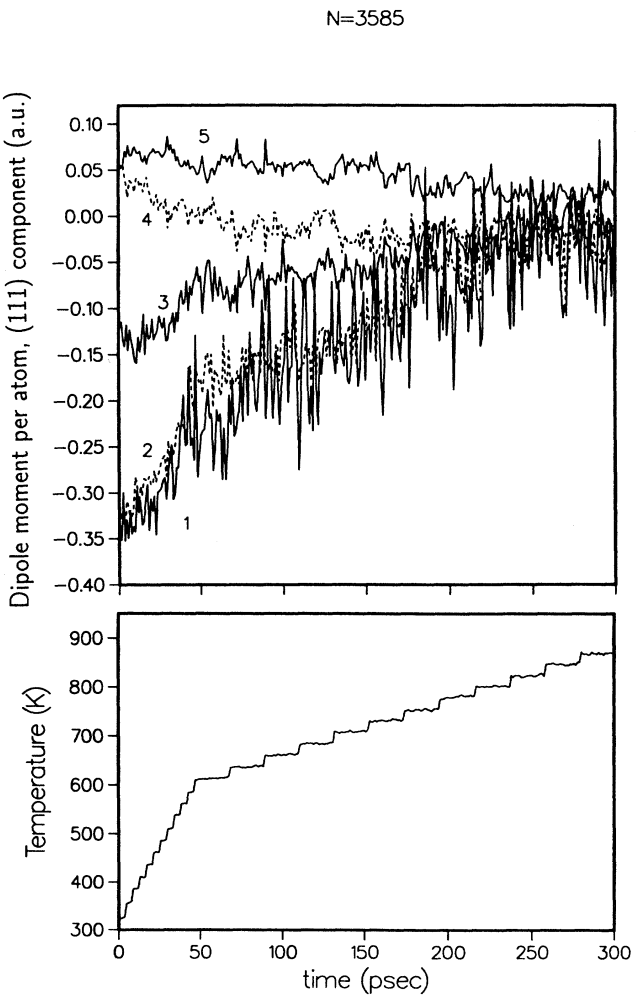

FIG. 5. The (111) component of the dipole moment per atom (atomic units) for each of the five shells (see Table I) of the 717 ($NaCaF_3$) cluster (upper panel) and the temperature (lower panel) as a function of simulation time.

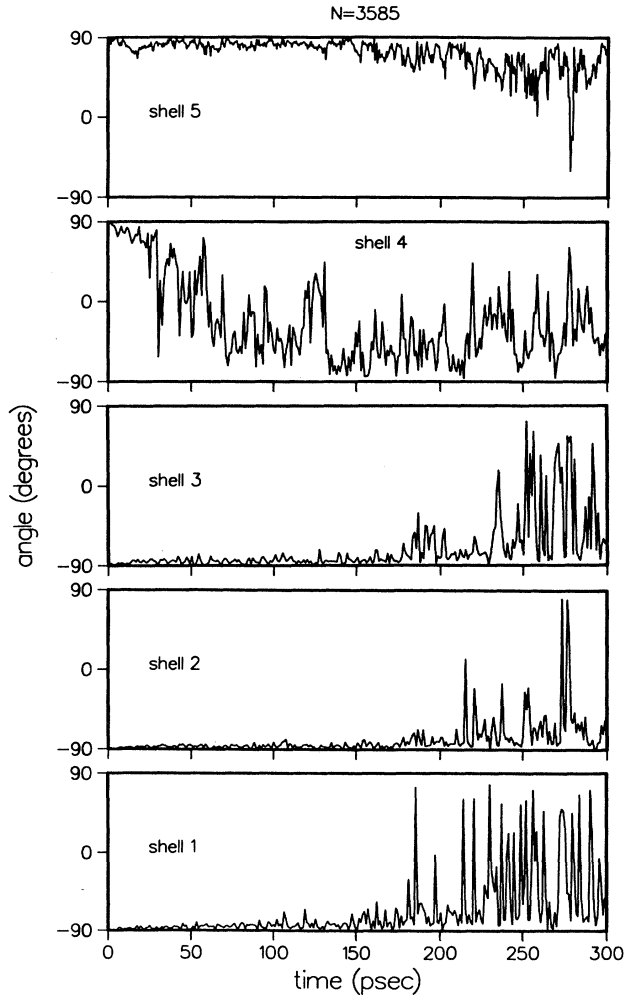

FIG. 6. Angle of the dipole moment of each shell of the 717 ($NaCaF_3$) cluster relative to the (111) axis as a function of simulation time [+90 corresponds to coincidence with the (111) direction].

for 3 and 4 at $t=0$) and moved into shell 4 after ~ 50 psec. The fluctuations of the inner shell dipole direction begin at ~ 180 psec, or just greater than 700 K.

D. $N=5900$

Results for the largest cluster considered reveal a more complicated initial domain structure than the smaller clusters. After a short simulation at low temperature ($T<400$ K) the outer shell (6) orients to $+90$, shell 5 remains at -90 throughout the entire simulation, shell 4 is evidently a transition region between the influence of shell 5 and the interior (shells 1, 2, and 3). The fluctuation of the polarization direction of the interior appears somewhat more pronounced than the smaller clusters; beginning at ~ 250 psec, it corresponds to a noticeably lower temperature (~ 630 K) than the smaller clusters.

VI. SUMMARY

The present calculations were motivated by (a) earlier calculations for $NaCaF_3$ which seemed to show ferroelectric behavior in clusters as small as $N\sim 1000$ and (b) reports of strong size-dependent effects on the ferroelectric transitions in $BaTiO_3$ and $PbTiO_3$. An algorithm for summing over pairwise interactions using a massively parallel computer was presented and a procedure for constructing stoichiometric clusters with no dipole moment from the perovskite structure was described. Our results show that the $NaCaF_3$ model has ferroelectric transitions for clusters larger than $N\sim 800$, in agreement with the earlier calculations. Contrary to the size-dependent effect in $BaTiO_3$ and $PbTiO_3$, the transition temperature in the $NaCaF_3$ model is somewhat larger for the clusters than

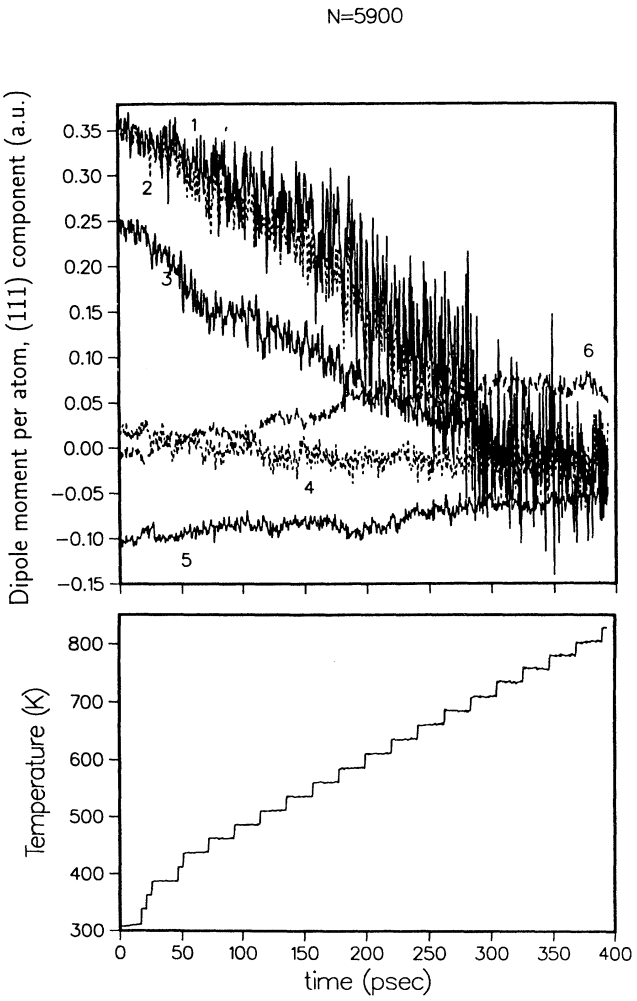

FIG. 7. The (111) component of the dipole moment per atom (atomic units) for each of the six shells (see Table I) of the 1180 ($NaCaF_3$) cluster (upper panel) and the temperature (lower panel) as a function of simulation time.

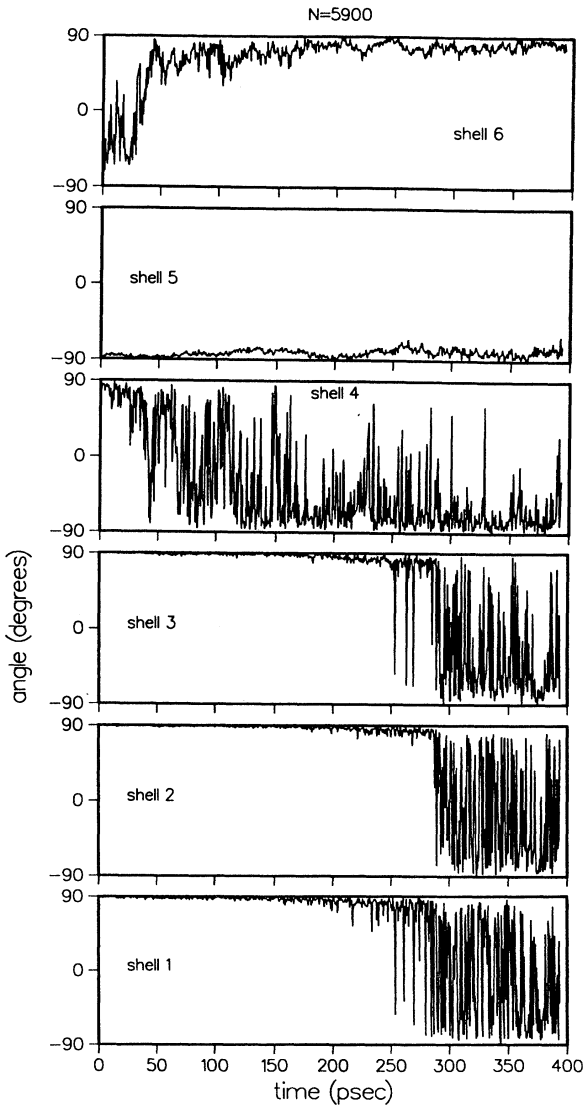

FIG. 8. Angle of the dipole moment of each shell of the 1180 ($NaCaF_3$) cluster relative to the (111) axis as a function of simulation time [+90 corresponds to coincidence with the (111) direction].

achieved in a "bulk" simulation. Together these results imply that the observed size-dependent effects in $BaTiO_3$ and $PbTiO_3$ derive somehow from the fundamental mechanism for ferroelectricity *in these systems,* rather than from some broader explanation. Factors which may be important in a detailed explanation are suggested by the differences between the origins of ferroelectricity in our model and in the real materials: (1) the ferroelectricity in $NaCaF_3$ is derived from rigid ions, while a more complex electronic mechanism is required to describe ferroelectricity in $BaTiO_3$ and $PbTiO_3$;[3] (2) $NaCaF_3$ is uniaxial in the paraelectric phase, while $BaTiO_3$ and $PbTiO_3$ have cubic paraelectric phases; (3) the ferroelectric instabilities in $BaTiO_3$ and $PbTiO_3$ are highly sensitive to volume with greater instability for larger volumes, while the instability for $NaCaF_3$ is less sensitive and decreases with volume.

ACKNOWLEDGMENTS

The author is grateful for helpful discussions with P. J. Edwardson and J. W. Flocken. This work was supported by the Office of Naval Research and, in part, by a grant of HPC time from the DoD HPC Shared Resource Center Naval Research Laboratory Connection Machines.

[1]Kenji Uchino, E. Sadanaga, and T. Hirose, J. Am. Ceram. Soc. **72**, 1555 (1989).

[2]P. J. Edwardson, L. L. Boyer, R. L. Newman, D. H. Fox, J. R. Hardy, J. W. Flocken, R. A. Guenther, and W. Mei, Phys. Rev. B **39**, 9738 (1989).

[3]R. E. Cohen, Nature (London) **358**, 137 (1992).

[4]D. J. Singh, in *Proceedings of the 3rd Williamsburg Workshop on First Principles Calculations For Ferroelectrics, Feb. 1994* [Ferroelectrics (to be published)].

[5]S. L. Swartz and V. E. Wood, Condens. Matter News **1**, 4 (1992).

[6]L. L. Boyer and J. R. Hardy, Phys. Rev. B **24**, 2577 (1981).

[7]L. L. Boyer, J. Phys. C **17**, 1825 (1984).

[8]L. L. Boyer and G. S. Pawley, J. Comp. Phys. **78**, 405 (1988).

[9]R. G. Gordon and Y. S. Kim, J. Chem. Phys. **56**, 3122 (1972).

[10]L. L. Boyer, Phys. Rev. B **23**, 3673 (1981).

[11]J. W. Flocken (private communication).

[12]P. J. Edwardson, V. Katkanant, J. R. Hardy, and L. L. Boyer, Phys. Rev. B **35**, 8470 (1987).

[13]L. L. Boyer and P. J. Edwardson, Ferroelectrics **104**, 417 (1990).